JCI The Journal of Clinical Investigation

TNF provokes cardiomyocyte apoptosis and cardiac remodeling through activation of multiple cell death pathways

Sandra B. Haudek, … , Michael D. Schneider, Douglas L. Mann

J Clin Invest. 2007;117(9):2692-2701. https://doi.org/10.1172/JCI29134.

Research Article **Cardiology**

Transgenic mice with cardiac-restricted overexpression of secretable TNF (MHCsTNF) develop progressive LV wall thinning and dilation accompanied by an increase in cardiomyocyte apoptosis and a progressive loss of cytoprotective Bcl-2. To test whether cardiac-restricted overexpression of Bcl-2 would prevent adverse cardiac remodeling, we crossed MHCsTNF mice with transgenic mice harboring cardiac-restricted overexpression of Bcl-2. Sustained TNF signaling resulted in activation of the intrinsic cell death pathway, leading to increased cytosolic levels of cytochrome *c*, Smac/Diablo and Omi/HtrA2, and activation of caspases -3 and -9. Cardiac-restricted overexpression of Bcl-2 blunted activation of the intrinsic pathway and prevented LV wall thinning; however, Bcl-2 only partially attenuated cardiomyocyte apoptosis. Subsequent studies showed that c-FLIP was degraded, that caspase-8 was activated, and that Bid was cleaved to t-Bid, suggesting that the extrinsic pathway was activated concurrently in MHCsTNF hearts. As expected, cardiac Bcl-2 overexpression had no effect on extrinsic signaling. Thus, our results suggest that sustained inflammation leads to activation of multiple cell death pathways that contribute to progressive cardiomyocyte apoptosis; hence the extent of such programmed myocyte cell death is a critical determinant of adverse cardiac remodeling.

TNF provokes cardiomyocyte apoptosis and cardiac remodeling through activation of multiple cell death pathways

Sandra B. Haudek,[1] George E. Taffet,[2] Michael D. Schneider,[3] and Douglas L. Mann[1,4]

[1]Winters Center for Heart Failure Research, [2]Section of Cardiovascular Sciences, and [3]Center for Cardiovascular Development, Department of Medicine, Baylor College of Medicine, Houston, Texas, USA. [4]Texas Heart Institute at St. Luke's Episcopal Hospital, Houston, Texas, USA.

Transgenic mice with cardiac-restricted overexpression of secretable TNF (MHCsTNF) develop progressive LV wall thinning and dilation accompanied by an increase in cardiomyocyte apoptosis and a progressive loss of cytoprotective Bcl-2. To test whether cardiac-restricted overexpression of Bcl-2 would prevent adverse cardiac remodeling, we crossed MHCsTNF mice with transgenic mice harboring cardiac-restricted overexpression of Bcl-2. Sustained TNF signaling resulted in activation of the intrinsic cell death pathway, leading to increased cytosolic levels of cytochrome *c*, Smac/Diablo and Omi/HtrA2, and activation of caspases -3 and -9. Cardiac-restricted overexpression of Bcl-2 blunted activation of the intrinsic pathway and prevented LV wall thinning; however, Bcl-2 only partially attenuated cardiomyocyte apoptosis. Subsequent studies showed that c-FLIP was degraded, that caspase-8 was activated, and that Bid was cleaved to t-Bid, suggesting that the extrinsic pathway was activated concurrently in MHCsTNF hearts. As expected, cardiac Bcl-2 overexpression had no effect on extrinsic signaling. Thus, our results suggest that sustained inflammation leads to activation of multiple cell death pathways that contribute to progressive cardiomyocyte apoptosis; hence the extent of such programmed myocyte cell death is a critical determinant of adverse cardiac remodeling.

Introduction

Transgenic mice with cardiac-restricted overexpression of TNF initially develop a concentric hypertrophic cardiac phenotype that segues to a dilated cardiac phenotype as the mice age, thus recapitulating the classic transition to failure that has been reported in many experimental models of cardiac decompensation (1–3). Recently we have shown that the development of LV wall thinning and adverse cardiac remodeling in mice with cardiac-restricted overexpression of secretable TNF (MHCsTNF mice) correlates with the prevalence of cardiomyocyte apoptosis (4). Another interesting observation that arose from these studies was that the prevalence of cardiomyocyte apoptosis increased in concert with an age-dependent decrease in the myocardial protein levels of Bcl-2, a critical member of the apoptosis-regulating protein family that suppresses cell death. This raised the intriguing possibility that sustained inflammatory signaling may have provoked progressive cardiomyocyte apoptosis as a result of the loss of one or more cytoprotective proteins. Two independent pathways may lead to cardiomyocyte apoptosis (reviewed in refs. 5, 6). The extrinsic (type I) pathway is initiated by ligands that bind to death receptors such as TNF receptor 1, whereas the intrinsic (type II) pathway is governed by the release of various proapoptotic proteins from the mitochondria. Whereas the inhibitors of apoptosis (IAPs) and cellular FLICE-like inhibitory protein (c-FLIP) prevent activation of the extrinsic pathway, Bcl-2 is a major regulator of mitochondrial membrane permeability and hence prevents activation of the intrinsic pathway. Although there is not complete agreement, the aggregate data suggest that the intrinsic, rather than extrinsic, death pathway is critical for cardiomyocyte fate decisions during heart failure (reviewed in refs. 5, 6).

The present study was undertaken in order to further delineate the role of cardiac apoptosis and cardiac remodeling in the MHCsTNF mice. Accordingly, we crossed the MHCsTNF mice with a previously reported line of mice harboring cardiac-restricted overexpression of human Bcl-2 (7) in order to determine whether overexpression of Bcl-2 in the heart would prevent cardiomyocyte apoptosis, as one would predict if myocytes behave as "type II cells." In mice with MHCsTNF mice loss of antiapoptotic proteins contributes to the activation of both intrinsic as well as extrinsic cell death pathways. Cardiac-restricted overexpression of Bcl-2 in the MHCsTNF mice attenuated cardiomyocyte apoptosis and LV remodeling by blocking the intrinsic cell death pathway, but did not prevent cardiac myocyte apoptosis secondary to activation of the extrinsic cell death pathway.

Results

Characterization of mouse models

Figure 1A shows that exogenous human Bcl-2 protein was readily detectable in cytosolic and mitochondrial extracts of hearts from Bcl-2 mice. Human Bcl-2 protein was also present in the myocardial cytosolic and mitochondrial extracts of the bitransgenic MHCsTNF/Bcl-2 mice, although at lower levels compared with Bcl-2 mice, consistent with the observation that TNF enhances Bcl-2 degradation (8). Human Bcl-2 protein was not detectable in myocardial extracts from littermate control

Nonstandard abbreviations used: c-FLIP, cellular FLICE-like inhibitory protein; c-FLIP$_L$, c-FLIP long isoform; c-FLIP$_S$, c-FLIP short isoform; c–IAP-1, cellular inhibitor of apoptosis 1; Endo G, endonuclease G; IAP, inhibitor of apoptosis; LVEDD, LV end-diastolic diameter; MHCsTNF mice, mice with cardiac-restricted overexpression of secretable TNF; r/h, ratio of LV radius to LV wall thickness; t-Bid, Bid cleaved to its truncated form.

Conflict of interest: The authors have declared that no conflict of interest exists.

Citation for this article: *J. Clin. Invest.* **117**:2692–2701 (2007). doi:10.1172/JCI29134.

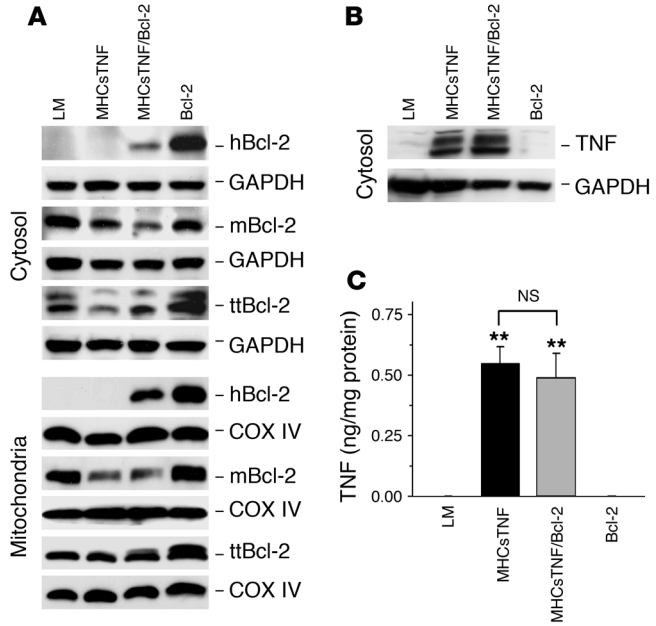

Figure 1
Characterization of mouse models. Representative Western blots showing (**A**) levels of exogenous human Bcl-2 (hBcl-2), endogenous mouse Bcl-2 (mBcl-2), and total (human and mouse) Bcl-2 (ttBcl-2) as well as (**B**) levels of mouse TNF in cytosolic and mitochondrial protein extracts of 12-week-old littermate control (LM), MHCsTNF, MHCsTNF/Bcl-2, and Bcl-2 mouse hearts. GAPDH (cytosol) and COX IV (mitochondria) served as loading normalization. (**C**) Myocardial TNF protein levels were measured by ELISA. $^{**}P < 0.05$ compared with LM.

(wild-type) and MHCsTNF hearts. As reported previously (4), cytosolic and mitochondrial levels of endogenous mouse Bcl-2 protein were lower in MHCsTNF than in littermate control hearts. Endogenous mouse Bcl-2 protein levels were also lower in MHCsTNF/Bcl-2 mice when compared with littermate controls and Bcl-2 mice. However, total (human and mouse) Bcl-2 levels in MHCsTNF/Bcl-2 hearts were comparable with Bcl-2 levels observed in littermate control hearts. Figure 1, B and C, shows that the level of myocardial TNF protein was not significantly different ($P = 0.51$) in the MHCsTNF and MHCsTNF/Bcl-2 mouse hearts ($n = 6$/group).

Effect of Bcl-2 on LV remodeling

We have shown previously that cardiomyocyte apoptosis contributes to the LV wall thinning in the MHCsTNF mice as they transition from a concentric hypertrophic phenotype at 4 weeks of age to a dilated phenotype at 12 weeks of age (1, 4). To determine whether overexpression of Bcl-2 was sufficient to attenuate adverse cardiac remodeling in the MHCsTNF mice, we examined cardiac structure using standard morphometric analyses and 2D-directed M-mode echocardiography in 4- and 12-week-old mice.

Table 1 shows that the heart weight–to–body weight ratios of the MHCsTNF and MHCsTNF/Bcl-2 mice at 4 and 12 weeks of age were both significantly greater than age-matched littermate control and Bcl-2 mice (4 wk, $n = 10$/group; 12 wk, $n = 12$/group) ($P < 0.001$). Although the heart weight–to–body weight ratio decreased significantly ($P < 0.02$) in the MHCsTNF and MHCsTNF/Bcl-2 mice from 4 to 12 weeks, there was no significant difference in the heart weight–to–body weight ratio between the MHCsTNF and MHCsTNF/Bcl-2 mice at either 4 or 12 weeks ($P > 0.54$). The increase in the heart weight–to–body weight ratio of the MHCsTNF and MHCsTNF/Bcl-2 relative to littermate control and Bcl-2 mice was not secondary to selective differences in body weight insofar as the body weights were not significantly different between groups of the same age ($P > 0.51$).

Figure 2A depicts representative echocardiograms for each group of mice at 12 weeks of age, whereas Figure 2, B–E, summarizes the results of group data (4 wk, $n = 6$/group; 12 wk, $n = 9$/group). Consistent with our prior observations (1, 4), the LV end-diastolic diameter (LVEDD) increased by 20% ($P < 0.001$) in the MHCsTNF mice from 4 to 12 weeks (Figure 2B). Although LVEDD increased in the MHCsTNF/Bcl-2 mice, this increase was smaller when compared with the change in LVEDD in the MHCsTNF mice. Thus at 12 weeks of age, the LVEDD in MHCsTNF/Bcl-2 mice was significantly lower ($P = 0.02$) than in the MHCsTNF mice. There was no difference in LVEDD between or within the littermate control and Bcl-2 mice at 4 and 12 weeks. Figure 2C shows that at 4 weeks of age, LV wall thickness in both MHCsTNF and MHCsTNF/Bcl-2 mice was significantly increased ($P < 0.001$) when compared with littermate control and Bcl-2 mice, although there was no difference between the MHCsTNF and MHCsTNF/Bcl-2 mouse groups. However, the salient finding shown by Figure 2C is that in MHCsTNF mice, LV wall thickness decreased by 16% ($P = 0.02$) from 4 to 12 weeks, whereas in the MHCsTNF/Bcl-2 mice there was no significant change in LV wall thickness during the same time period. As a result, the absolute LV wall thickness at 12 weeks of age was 32% higher ($P < 0.001$) in MHCsTNF/Bcl-2 mice when compared with MHCsTNF mice. The increase in LVEDD and LV wall thinning resulted in a 44% increase ($P < 0.001$) in the ratio of LV radius to LV wall thickness (r/h) in the MHCsTNF mice from 4 to 12 weeks (Figure 2D), consistent with adverse cardiac remodeling. By comparison, the r/h ratio remained relatively unchanged in the MHCsTNF/Bcl-2 from 4 to 12 weeks, and thus, at 12 weeks of age the r/h ratio of MHCsTNF/Bcl-2 mice was 29% lower ($P < 0.001$) than that of the MHCsTNF mice, suggesting that overexpression of Bcl-2 prevented adverse cardiac remodeling in the MHCsTNF mice. In addition, while the percent of fractional shortening (%FS)

Table 1
Effect of Bcl-2 on cardiac hypertrophy

	LM	MHCsTNF	MHCsTNF/Bcl-2	Bcl-2
HW/BW 4 wk	4.57 ± 0.10	6.19 ± 0.18^{A}	6.02 ± 0.16^{A}	4.43 ± 0.10
HW/BW 12 wk	4.23 ± 0.18	5.28 ± 0.23^{A,B}	5.41 ± 0.26^{A,B}	4.22 ± 0.11
BW (g) 4 wk	20.2 ± 1.0	19.3 ± 1.3	19.0 ± 0.8	19.9 ± 1.4
BW (g) 12 wk	30.8 ± 1.9^{B}	32.0 ± 1.2^{B}	32.0 ± 1.2^{B}	30.1 ± 1.7^{B}

Body and heart weights from littermate control (LM), MHCsTNF, MHCsTNF/Bcl-2, and Bcl-2 mice were recorded at 4 and 12 weeks of age. Data are shown as mean ± SEM for the actual heart weight–to–body weight ratio (HW/BW) and body weight (BW). Overexpression of Bcl-2 in the heart did not reduce cardiac hypertrophy in MHCsTNF mice. $^{A}P < 0.05$ compared with LM; $^{B}P < 0.05$ between 4 and 12 weeks of age within the same transgenic mouse line.

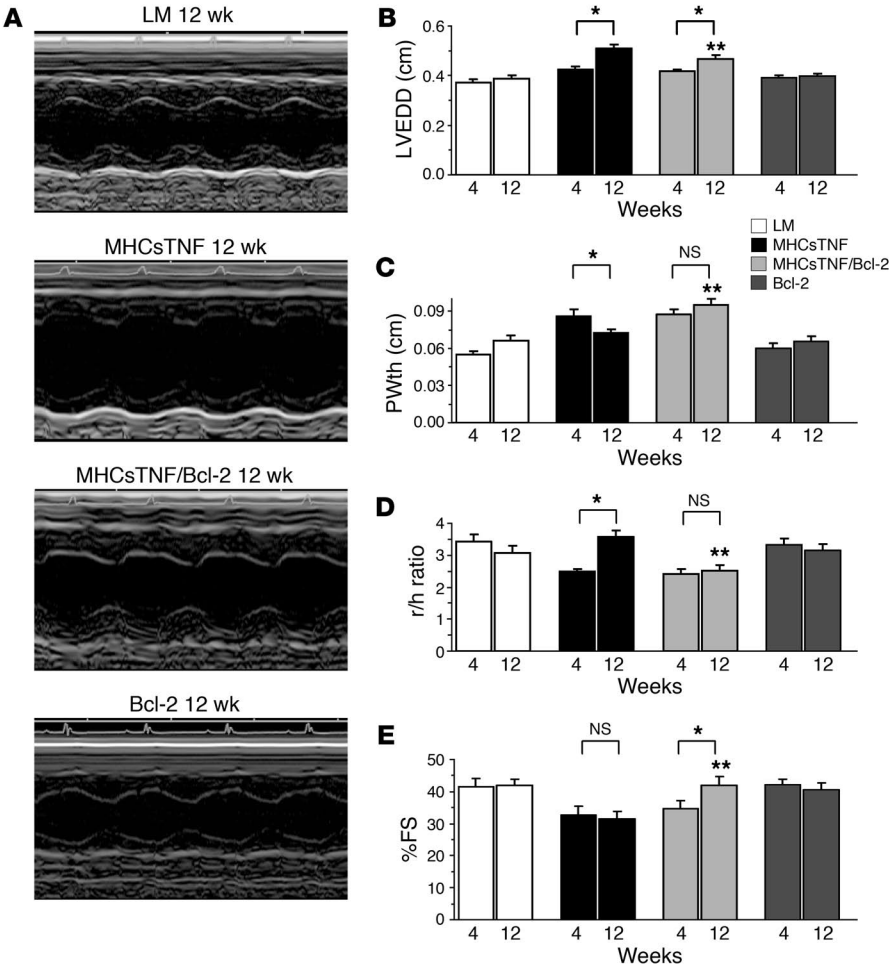

Figure 2
Effect of Bcl-2 on LV remodeling. (**A**) Representative M-mode echocardiograms for littermate control, MHCsTNF, MHCsTNF/Bcl-2, and Bcl-2 mouse hearts. Group data for (**B**) LVEDD, (**C**) posterior wall thickness (PWth), (**D**) r/h, and (**E**) percent fractional shortening (%FS) for LM, MHCsTNF, MHCsTNF/Bcl-2, and Bcl-2 mouse hearts. *P < 0.05 between 4 and 12 weeks of age within the same transgenic mouse line; **P < 0.05 between MHCsTNF and MHCsTNF/Bcl-2 at 12 weeks of age.

in MHCsTNF mice remained significantly lower (P < 0.01) than age-matched littermate controls from 4 to 12 weeks, the %FS in MHCsTNF/Bcl-2 mice increased significantly (P < 0.05) during the same time period (Figure 2E). Thus, at 12 weeks of age the %FS in MHCsTNF/Bcl-2 mice was 33% higher (P < 0.01) than in the MHCsTNF mice and was not significantly different from littermate control and Bcl-2 mice, suggesting that overexpression of Bcl-2 prevented the decrease in contractile dysfunction observed in the MHCsTNF mice.

Cardiomyocyte apoptosis

We have shown that the prevalence of cardiomyocyte apoptosis increases in a time-dependent manner in the MHCsTNF mice and that this increase in apoptosis is accompanied by a progressive loss of myocardial Bcl-2 and a concomitant increase in the release of cytochrome *c* from the mitochondria into the cytosol (4). Given that TNF enhances Bcl-2 degradation (8), these initial observations suggested a role for TNF-induced activation of the intrinsic cell death pathway in the adverse cardiac remodeling that we observed in the MHCsTNF mice. To determine whether cardiac overexpression of Bcl-2 was sufficient to attenuate apoptosis in the MHCsTNF/Bcl-2 mice, we compared the prevalence of apoptotic cardiac nuclei in 12-week-old MHCsTNF/Bcl-2 mice to MHCsTNF mouse hearts using the in situ DNA ligase technique (4, 9). Figure 3 shows that the prevalence of cardiomyocyte apoptosis was 60% lower (P = 0.001) in MHCsTNF/Bcl-2 mice than in MHCsTNF mice (n = 5/group). Importantly, however, cardiac overexpression of Bcl-2 did not completely abrogate cardiomyocyte apoptosis in MHCsTNF mice since the prevalence of apoptosis in MHCsTNF/Bcl-2 mouse hearts was still significantly greater (P < 0.001) than in Bcl-2 or littermate control hearts.

Mechanisms for cardiomyocyte apoptosis: intrinsic pathway

Myocardial cytochrome c release. To investigate the mechanism(s) responsible for the Bcl-2–mediated attenuation of cardiomyocyte apoptosis we first examined mitochondrial release of cytochrome *c* in the hearts of 12-week-old MHCsTNF and MHCsTNF/Bcl-2 mouse hearts. Representative Western blots of mitochondrial and cytosolic levels of cytochrome *c* are depicted in Figure 4, A and B. Reprobing the membranes for both GAPDH and cytochrome *c* oxidase subunit IV showed that the cytosolic and mitochondrial protein extracts were relatively pure and that protein loading was equal. Analysis of the group data shown in Figure 4, A and B, showed that in MHCsTNF mouse hearts, mitochondrial cytochrome *c* levels were significantly lower (P < 0.01) and cytosolic cytochrome *c* levels were significantly higher (P < 0.01) than the corresponding cytochrome *c* levels in littermate control and Bcl-2 hearts (n = 12/group). Importantly, in MHCsTNF/Bcl-2 hearts, mitochondrial cytochrome *c* levels were significantly higher (P < 0.01) and cytosolic cytochrome *c* levels were significantly lower (P < 0.05) than in MHCsTNF hearts and were not different from the corresponding levels in littermate control and Bcl-2 mice.

Myocardial levels of proapoptotic proteins. To further explore the effects of Bcl-2 overexpression in the heart, we examined protein levels of several mitochondrial apoptogens. Figure 5A shows representative Western blots for proapoptotic Smac/Diablo, Omi/HtrA2, apoptosis inducing factor (AIF), and endonuclease G (Endo G) in 12-week-old mice. As shown by the corresponding group data in Figure 5B, the cytosolic levels of Smac/Diablo (n = 16/group) and Omi/HtrA2 (n = 8/group) were significantly higher (P < 0.001) in the hearts of the MHCsTNF mice relative to littermate control and Bcl-2 mice. Importantly, overexpression of Bcl-2 in cardiomyocytes led to a significant reduction (P < 0.01

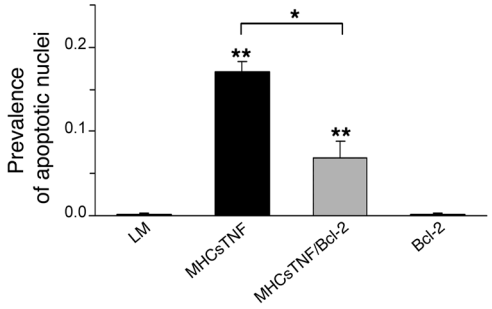

Figure 3
Cardiomyocyte apoptosis. The prevalence of cardiomyocyte apoptosis was determined by the in situ DNA ligation method in littermate control, MHCsTNF, MHCsTNF/Bcl-2, and Bcl-2 mouse hearts at 12 weeks of age. *$P < 0.05$ between MHCsTNF and MHCsTNF/Bcl-2 mice; **$P < 0.05$ compared with LM.

relative to MHCsTNF mice) in the release of these 2 proapoptotic proteins. Although the levels of Omi/HtrA2 were reduced to baseline levels in the MHCsTNF/Bcl-2 mouse hearts, the levels of Smac/Diablo were still greater than those observed in littermate control and Bcl-2 mice. The cytosolic levels of AIF ($n = 16$/group) and Endo G ($n = 12$/group) were not different ($P = 0.3$ and 0.4, respectively) in the hearts of MHCsTNF, MHCsTNF/Bcl-2, Bcl-2, and littermate control mice.

Myocardial caspase-3 and -9 activation. To determine whether cardiac-restricted overexpression of Bcl-2 decreased activation of caspases that have been implicated in the intrinsic cell death pathway, we measured caspase-3– and caspase-9–like activities in the hearts of 12-week-old MHCsTNF and MHCsTNF/Bcl-2 mice. Figure 6, A and B, shows that caspase-3–and caspase-9–like activity were significantly increased ($P < 0.001$) in myocardial extracts from the MHCsTNF mice relative to littermate controls ($n = 8$/group). Although caspase-3– and caspase-9–like activity were both significantly reduced in the MHCsTNF/Bcl-2 mice when compared with the MHCsTNF mice ($P < 0.001$ and $P = 0.03$, respectively), the levels of caspase-3– and caspase-9–like activity were still significantly ($P < 0.05$) greater than those observed in the littermate control and Bcl-2 mice.

Mechanisms for cardiomyocyte apoptosis: extrinsic pathway
Given that cardiac-restricted overexpression of Bcl-2 was sufficient to prevent mitochondrial cytochrome *c* release but did not completely abrogate apoptosis in the MHCsTNF/Bcl-2 mice, we asked whether the extrinsic, Bcl-2–insensitive pathway was activated as well.

Myocardial caspase-8 activation, Bid, IAPs, and c-FLIP. Figure 7A shows that caspase-8–like activity was significantly greater ($P < 0.001$) in the MHCsTNF hearts when compared with littermate control and Bcl-2 mice ($n = 8$/group). Importantly, the levels of caspase-8–like activation were not different in the MHCsTNF and MHCsTNF/Bcl-2 mice ($P = 0.16$). The representative Western blot illustrated in Figure 7B shows that full-length Bid (23 kDa) was present in the cytosolic extracts of the littermate control and Bcl-2 mice, whereas Bid was cleaved to its truncated form (t-Bid; 15 kDa) in MHCsTNF as well in MHCsTNF/Bcl-2 mice. The group data shown in Figure 7B show that cytosolic full-length Bid was significantly decreased ($P < 0.01$) in the MHCsTNF and MHCsTNF/Bcl-2 mice when compared with littermate control and Bcl-2 mice ($n = 8$/group). Moreover, cytosolic t-Bid was significantly increased ($P < 0.01$) in the MHCsTNF and the MHCsTNF/Bcl-2 mice when compared with the control groups ($n = 8$/group). There was no difference in myocardial t-Bid levels between the MHCsTNF and the MHCsTNF/Bcl-2 mice, consistent with the lack of effect of Bcl-2 on caspase-8 activation. Another important finding shown by Figure 7C is that the levels of cellular inhibitor of apoptosis 1 (c–IAP-1) were significantly ($P < 0.001$) reduced in the MHCsTNF mice relative to littermate controls ($n = 12$/group), indicating that sustained expression of TNF induced loss of cytoprotective c–IAP-1.

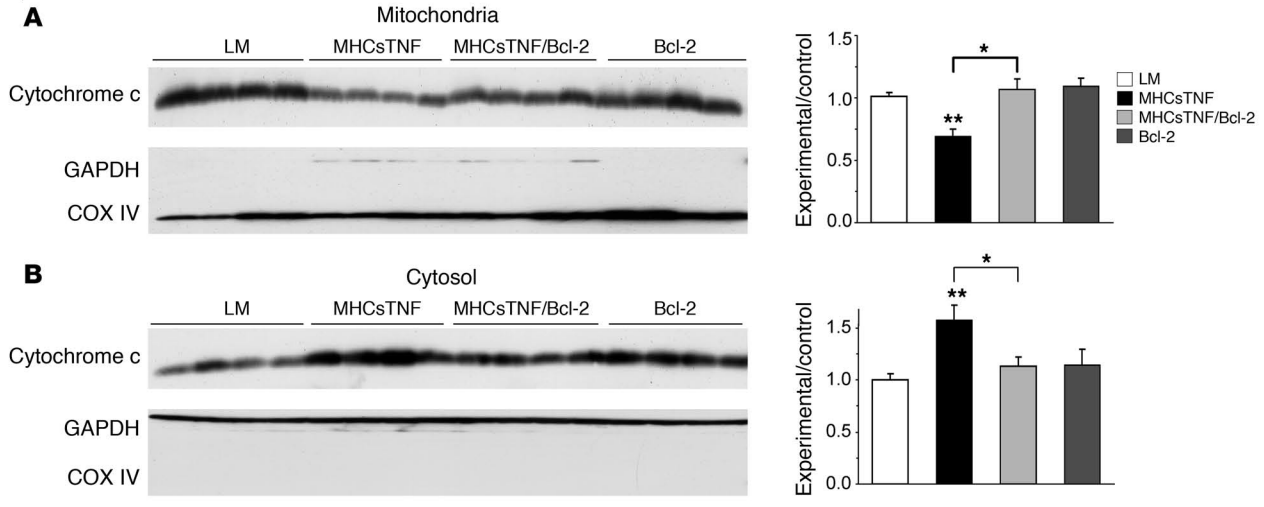

Figure 4
Myocardial cytochrome *c* release. The release of cytochrome *c* from (**A**) mitochondria to (**B**) the cytosol was determined by Western blotting in 12-week-old littermate control, MHCsTNF, MHCsTNF/Bcl-2, and Bcl-2 mouse hearts. Shown are representative Western blots next to the group data for mitochondrial cytochrome *c* levels (normalized to COX IV) and cytosolic cytochrome *c* levels (normalized to GAPDH). Group data represent the ratio of experimental (transgenic) to control (wild-type) mouse groups. *$P < 0.05$ between MHCsTNF and MHCsTNF/Bcl-2 groups; **$P < 0.05$ compared with LM.

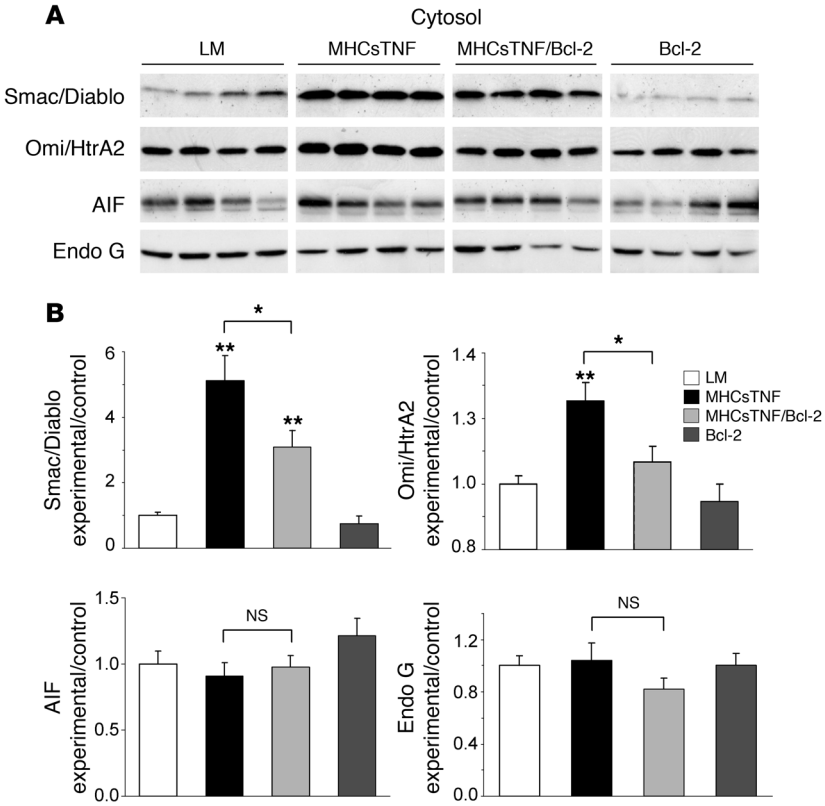

Figure 5
Myocardial levels of proapoptotic proteins. (**A**) The release of mitochondrial Smac/Diablo, Omi/HtrA2, apoptosis-inducing factor (AIF), and Endo G into the cytosol was determined by Western blotting in littermate control, MHCsTNF, MHCsTNF/Bcl-2, and Bcl-2 mouse hearts at 12 weeks of age. (**B**) Group data for the corresponding protein levels (normalized to GAPDH) are expressed as the ratio of experimental (transgenic) to control (wild-type) mouse groups. **P* < 0.05 between MHCsTNF and MHCsTNF/Bcl-2 groups; ***P* < 0.05 compared with LM.

However, cardiac overexpression of Bcl-2 did not prevent the TNF-induced decrease in the level of c–IAP-1. In contrast, there was no difference ($P = 0.43$) in the cytosolic levels of c–IAP-2 in the MHCsTNF/Bcl-2 mice relative to levels in the MHCsTNF, littermate control, and Bcl-2 mice ($n = 12$/group).

Noting a recent report that showed that TNF-mediated activation of JNK resulted in ubiquitination and degradation of c-FLIP long isoform (c-FLIP$_L$), an inhibitor of caspase-8 (10), we sought to determine whether there were differences in the level of c-FLIP$_L$ in the hearts of the MHCsTNF and/or MHCsTNF/Bcl-2 mice. Figure 8A depicts representative Western blots and resulting group data for the protein levels of cardiac c-FLIP$_L$ and of its isoform c-FLIP short isoform (c-FLIP$_s$) in MHCsTNF and MHCsTNF/Bcl-2 mice. As shown, both c-FLIP$_L$ and c-FLIP$_s$ protein levels were significantly ($P < 0.01$) reduced in MHCsTNF mice relative to littermate control and Bcl-2 mice ($n = 8$/group). Moreover, protein levels for c-FLIP$_L$ and c-FLIP$_s$ were not different in the MHCsTNF and the MHCsTNF/Bcl-2 mice ($P = 0.8$ and 0.2, respectively). To determine whether the decrease in c-FLIP$_L$ levels related to decreased c-FLIP$_L$ mRNA levels, we performed RNase protection assays. As shown in Figure 8B, there was no significant difference ($P = 0.29$) in the mRNA levels of *c-FLIP$_L$* in the hearts of the littermate control, MHCsTNF, MHCsTNF/Bcl-2, and Bcl-2 mice ($n = 8$/group).

Discussion

Cardiac remodeling contributes to the development and progression of heart failure (reviewed in ref. 11). However, the mechanisms that contribute to the structural changes that underlie progressive cardiac remodeling are only partially understood. Recent studies have shown that forced expression of components of either the extrinsic or intrinsic cell death pathways provokes a dilated cardiac phenotype in the adult heart (12, 13), suggesting that programmed myocyte cell death may contribute to progressive cardiac decompensation. In support of this point of view, studies that have used broad-based caspase inhibitors to prevent myocyte apoptosis have demonstrated that cardiac remodeling is attenuated in lines of transgenic mice with forced cardiac overexpression of Gαq and TNF (4, 14). However, caspases can degrade myofibrillar proteins and transcription factors responsible for the expression of muscle genes in myocytes (15, 16). In addition, caspases can inhibit the ubiquitin proteasome system that is responsible for recycling peptides obtained from degraded myofibrillar proteins (17). Thus, the aforementioned studies with caspase inhibitors

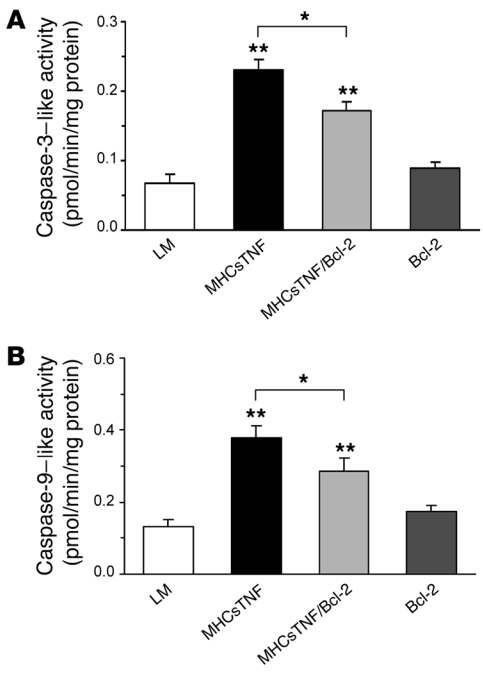

Figure 6
Myocardial caspase-3 and -9 activation. (**A**) Caspase-3–like and (**B**) caspase-9–like activities were determined in 12-week-old littermate control, MHCsTNF, MHCsTNF/Bcl-2, and Bcl-2 mouse hearts using a fluorogenic assay. **P* < 0.05 between MHCsTNF and MHCsTNF/Bcl-2 groups; ***P* < 0.05 compared with LM.

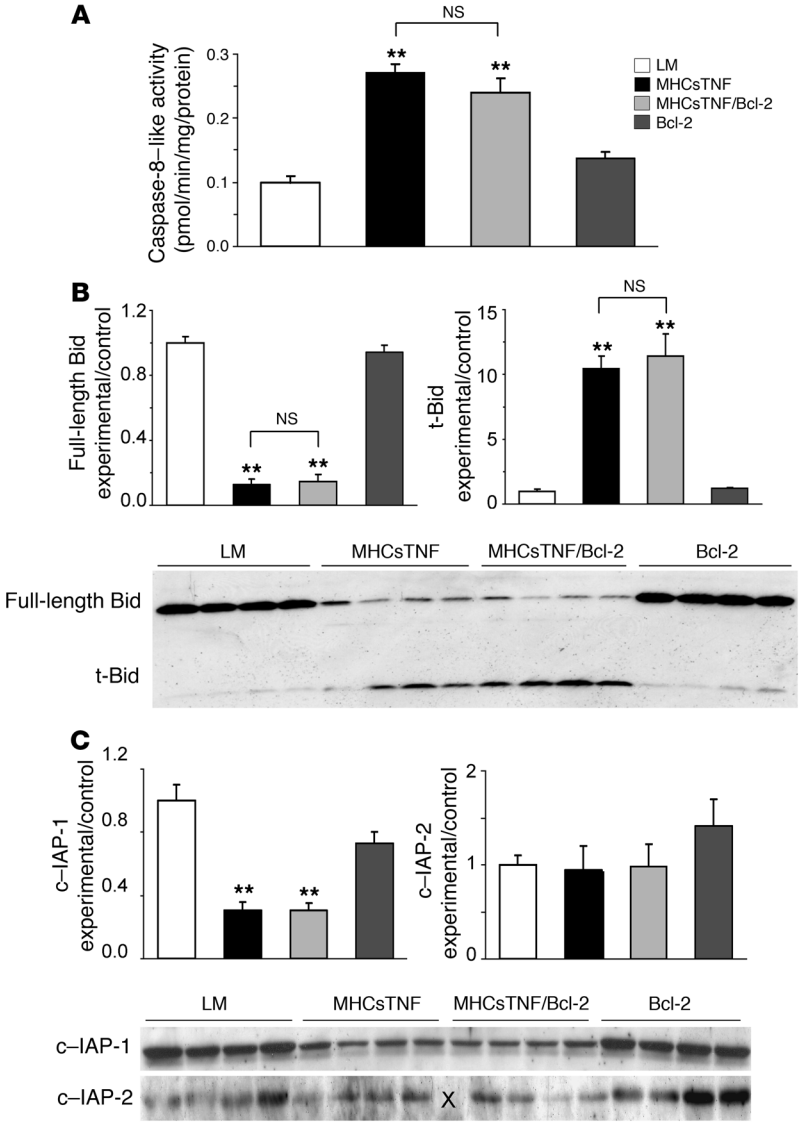

Figure 7
Myocardial caspase-8 activation, Bid, and IAPs. (**A**) Caspase-8–like activity was determined in 12-week-old littermate control, MHCsTNF, MHCsTNF/Bcl-2, and Bcl-2 mouse hearts using a fluorogenic assay. Cytosolic levels of (**B**) full-length Bid (23 kDa) and t-Bid (15 kDa) and of (**C**) c–IAP-1 and c–IAP-2 as determined by Western blotting. Group data for the corresponding levels (normalized to GAPDH) are shown as the ratio of experimental (transgenic) to control (wild-type) mouse groups. x, empty lane. *$P < 0.05$ compared with LM.

cannot be used as unambiguous evidence in support of the contribution of programmed cell death to progressive cardiac remodeling.

Here we have taken a genetic approach to inhibit cardiomyocyte apoptosis in mice overexpressing TNF in the cardiac compartment. Results from the present study show for the first time that cardiac overexpression of Bcl-2 not only reduces the prevalence of TNF-induced cardiomyocyte apoptosis in bitransgenic MHCsTNF/Bcl-2 mice (Figure 3) but also prevents the LV wall thinning, the adverse cardiac remodeling (increased r/h ratio), and the decrease in fractional shortening that occurs in these mice (Figure 2) from 4 to 12 weeks of age. From a pathophysiological standpoint, the increase in LV wall thinning that attends progressive cardiomyocyte apoptosis would be expected to contribute to increased LV wall stress (i.e., afterload mismatch) and hence sustained unfavorable loading conditions of the heart, thereby contributing to progressive cardiac decompensation. Indeed, using a similar transgenic approach we have previously shown that Bcl-2 overexpression prevented cardiac hypertrophy and improved cardiac function in desmin-null mice that develop cardiomyopathy (18).

In addition to clarifying the role of cardiomyocyte apoptosis with respect to cardiac remodeling, the results of this study provide several new insights into the mechanisms that contribute to programmed cardiomyocyte cell death in vivo. As noted at the outset, we have observed an increased prevalence of apoptosis in the MHCsTNF mice as they age from 4 to 12 weeks. As reported previously, apoptosis in the MHCsTNF mice was primarily observed in cardiomyocytes, in contrast to other studies wherein cardiac-restricted overexpression of TNF was shown to lead to apoptosis in interstitial and inflammatory cells (2–4). This increased prevalence of apoptosis cannot be explained by increasing levels of myocardial TNF in the MHCsTNF mice with age; in fact we have previously reported decreased levels of myocardial TNF in the older MHCsTNF mice, perhaps related to α-myosin heavy chain promoter activity (1). A more likely explanation is that sustained TNF signaling in some way allows the myocytes to become more sensitive to the proapoptotic effects of TNF over time. Several lines of evidence support this intriguing point of view. First, sustained TNF signaling resulted in progressive depletion of cytoprotective proteins that prevent the activation of both the intrinsic (Bcl-2) and the extrinsic (c-FLIP, c–IAP-1) cell death pathways. Second, progressive loss of Bcl-2 in the MHCsTNF mice contributed to the mitochondrial release of cytochrome *c*, Smac/Diablo, and Omi/HtrA2 into the cytosol (Figures 4 and 5). In keeping with this point of view, overexpression of Bcl-2 restored cytosolic levels of cytochrome *c* and Omi/HtrA2 to those observed in littermate control mice. The mitochondrial release of Smac/Diablo as well as levels of caspase-9 activity were significantly reduced in the MHCsTNF/Bcl-2 mice, even though their levels were not reduced to baseline levels. Although the reason for this finding is not known, one possibility is that the levels of Bcl-2 in MHCsTNF/Bcl-2 were inadequate to normalize the release of mitochondrial apoptogens such as Smac/Diablo (Figure 5). Elevated levels of cytosolic Smac/Diablo would be expected to promote amplification of the intrinsic and extrinsic cell death pathways by preventing the IAPs from blunting caspase-3 activation (see Figure 9) (19). Alternatively, other Bcl-2–independent mechanisms such as the extrinsic apoptotic pathway may have contributed to the observed cardiomyocyte cell death. Recent studies have demonstrated that the TNF-induced extrinsic cell death pathway involves the formation of 2 sequential signaling

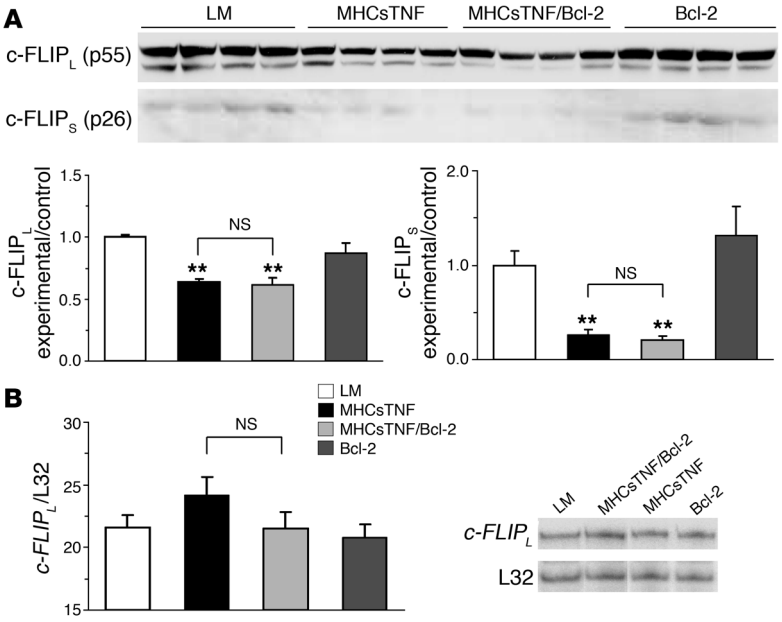

Figure 8
Myocardial c-FLIP$_L$ and C-FLIP$_S$ levels. (**A**) Cytosolic protein levels of c-FLIP$_L$ and c-FLIP$_S$ were determined in 12-week-old littermate control, MHCsTNF, MHCsTNF/Bcl-2, and Bcl-2 mouse hearts by Western blotting. Group data for the corresponding protein levels (normalized to GAPDH) are shown as the ratio of experimental (transgenic) to control (wild-type) mouse groups. (**B**) *c-FLIP$_L$* mRNA levels were determined by RNase protection assay, and representative results as well as group data (normalized to L32) are shown. $^{**}P < 0.05$ compared with LM.

complexes termed "complex I" and "complex II" (see Figure 9) (20). Engagement of TNF receptor superfamily, member 1 (TNFR1) by TNF ligand leads to recruitment of the death domain–containing proteins TNFR1-associated via death domain (TRADD) and TNFR-interacting serine-threonine kinase 1 (RIP1), which can then participate in either complex I or complex II. Complex I, which contains TNFR-associated factor 2 (TRAF2), binds to the cytoplasmic tail of TNFR1 and promotes the activation of the cytoprotective transcription factor NF-κB as well as activation of JNK. The balance between NF-κB and JNK activation is critical for cell fate. Complex II is assembled when TRADD and RIP1 are ubiquitinated and localize to the cytosol, where they associate with Fas-associated death domain (FADD) and caspase-8. When NF-κB is activated by complex I, complex II harbors the caspase-8 inhibitor c-FLIP$_L$, and the cell survives. However, when c-FLIP$_L$ is degraded, such as by JNK activation (10), and is absent from complex II, cell death proceeds through processing of caspase-8, with resultant activation of distal effector caspases such as caspase-3. The decreased levels of c-FLIP$_L$ protein in the MHCsTNF and the MHCsTNF/Bcl-2 mice may have allowed for the activation of caspase-8 within complex II as well as the cleavage of Bid to t-Bid (Figure 7) with subsequent mitochondrial release of proapoptotic factors that amplified the activation of the downstream intrinsic pathway (21). Nonetheless, it should be recognized that the data linking decreased levels of c-FLIP$_L$ to increased activation of the extrinsic cell death pathway is correlative and therefore should be regarded as provisional. Although we did not determine the exact mechanism for the loss of c-FLIP$_L$ protein in the MHCsTNF and MHCsTNF/Bcl-2 mice, the observation that the levels of *c-FLIP$_L$* mRNA were not decreased (Figure 8) is consistent with observations that TNF-mediated JNK activation accelerates ubiquitination and degradation of c-FLIP$_L$ (10).

In addition to blocking the release of apoptotic factors (22), Bcl-2 may be cytoprotective by inhibiting the mitochondrial permeability transition pore (23) and enhancing the rate of oxidative phosphorylation by attenuating the mitochondrial Na^+-Ca^{2+} exchanger (and hence preventing mitochondrial calcium matrix efflux) (24) as well as by reducing the rate of ATP decline and intracellular acidification during ischemia by directly inhibiting F1F0-ATPase (25). In addition, Bcl-2 exerts antiapoptotic effects through an NF-κB–dependent (26) and/or antioxidant mechanism(s) (27) and by inhibiting proapoptotic JNK activation (28) in ventricular myocytes. Thus, we cannot exclude caspase-independent effects of Bcl-2 in our model. Lastly, since cardiac-restricted overexpression of Bcl-2 alone was not sufficient to abrogate the adverse remodeling in MHCsTNF mice, it is likely there are other mechanisms that contribute to cardiomyocyte apoptosis in the MHCsTNF mice. In parallel studies we have determined that decreased vascularization and/or decreased numbers of proliferating cardiomyocytes

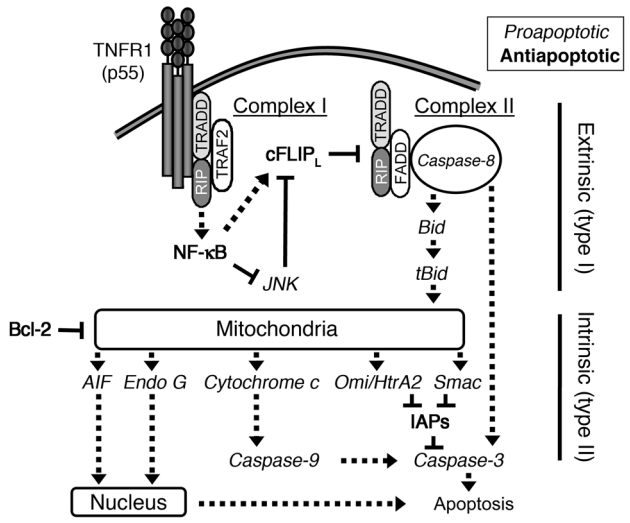

Figure 9
Pro- and anti-apoptotic proteins that govern the extrinsic and intrinsic cell death pathways. Proapoptotic proteins are shown in italic, antiapoptotic proteins in bold. TNF-induced signaling involves the formation of 2 sequential signaling complexes, complex I and complex II. Complex I is bound to TNF receptor superfamily, member 1 (TNFR1) and contains TNFR1-associated death domain (TRADD), TNFR-interacting serine-threonine kinase (RIP), and TNFR-associated factor 2 (TRAF2). Complex II is located in the cytosol and contains TRADD, RIP1, Fas-associated death domain (FADD), and caspase-8. See Discussion for further details.

were unlikely to explain the adverse remodeling in the MHCsTNF mice (see Supplemental Figure 1; supplemental material available online with this article; doi:10.1172/JCI29134DS1). Moreover, we have shown that the broad-based matrix metalloproteinase inhibitor abrogated LV dilation but had no effect on LV wall thickness in a similar line of mice with cardiac-restricted overexpression of TNF (29). Thus adverse remodeling in the MHCsTNF mice likely represents the consequence of increased wall thinning secondary to apoptosis and matrix degradation secondary to activation of matrix metalloproteinases.

Conclusion

The results of this study, in which we have taken a genetic approach to inhibit programmed cell death, suggest that the development of progressive cardiomyocyte apoptosis plays a critical role in the LV wall thinning and adverse cardiac remodeling that occur in the setting of sustained inflammation. This study further suggests that the biological processes that govern cardiomyocyte cell death in vivo are far more complex than have been proposed (12, 13). That is, our results suggest that in vivo, apoptotic cell death does not necessarily occur as a direct result of the activation of the cell death pathways per se but rather that cell death proceeds after sustained TNF signaling renders myocytes competent to die, after one or more antiapoptotic cytoprotective proteins are depleted (see Figure 9). Indeed, our prior observation that progressive loss of Bcl-2 protein correlates with the increasing prevalence of cardiomyocyte apoptosis in the MHCsTNF mice, (4) coupled with the observation in the present study that cardiac overexpression of Bcl-2 is sufficient to partially attenuate apoptosis and abrogate LV wall thinning in the MHCsTNF/Bcl-2 mice, is entirely consistent with this point of view. In this regard, in future studies it will be extremely important to determine whether progressive depletion of the antiapoptotic cytoprotective proteins that regulate the intrinsic and/or extrinsic cell death pathways favors activation of these pathways in a "feed-forward" self-amplifying manner that renders cells progressively more competent to die in the setting of sustained cardiac injury and/or inflammation.

Methods

Characterization of mouse models

The generation and characterization of the line of transgenic mice with cardiac-restricted overexpression of secretable TNF (referred to as MHCsTNF mice) in a C57BL/6 background has been described in detail (1, 30). Transgenic mice with cardiac-restricted overexpression of human Bcl-2 (Bcl-2 mice) were generated in a FVB/N background as previously described (7). Both mouse lines were hemizygous for their respective transgene. Male MHCsTNF mice were crossbred with female Bcl-2 mice to generate bitransgenic MHCsTNF/Bcl-2 mice. The resulting F1 offspring was genotyped by PCR in order to separate the MHCsTNF and MHCsTNF/Bcl-2 mice from the littermate control and Bcl-2 mice. All control mice (wild-type and Bcl-2) were the respective littermates of MHCsTNF and MHCsTNF/Bcl-2 mice. Both male and female (~1:1) offspring was used for experiments. The level of Bcl-2 protein expression in the littermate control, MHCsTNF, MHCsTNF/Bcl-2, and Bcl-2 mice were examined at 12 weeks by Western blotting, using monoclonal anti-human Bcl-2 and monoclonal anti-mouse Bcl-2 (both from BD Biosciences — Pharmingen), and polyclonal anti-human/anti-mouse Bcl-2 (Santa Cruz Biotechnology Inc.) antibodies. The level of myocardial TNF in the mouse lines was determined by Western blotting using a polyclonal anti-mouse TNF antibody (Abcam Inc.) and by ELISA as previously described (1, 30). All experiments were approved by the Institutional Animal Care and Use Committee of Baylor College of Medicine. All animals were used in accordance with the guidelines of the Baylor College of Medicine Animal Care and Research Advisory Committee and in accordance with the rules governing animal use, as published by the NIH.

Effect of Bcl-2 on LV remodeling

Structural data on mouse hearts were obtained by 2D-directed M-mode echocardiography at 4 and 12 weeks of age as previously described, using an Acuson Sequoia Cardiac System equipped with 15-MHz linear transducer (C256 and 15L8; Acuson Co.) (31). All images were digitally acquired and stored for offline analysis. Mice were euthanized after imaging and body and heart weights were recorded.

Cardiomyocyte apoptosis

Hearts were excised from the littermate control, MHCsTNF, MHCsTNF/Bcl-2, and Bcl-2 mice at 12 weeks of age and perfusion fixed with 10% zinc-buffered formalin. Fixed hearts were embedded in paraffin, and 6 μm myocardial sections were fixed onto glass slides. Apoptotic cardiomyocytes were identified on paraffin-embedded myocardial sections using the in situ DNA ligation technique that labels cell nuclei containing double-stranded DNA breaks with single-base 3′ overhangs as previously described (4, 9). Apoptotic cell nuclei detected by the ligase assay were stained with fluorescein (excitation/transmission wavelength, 495/525 nm). Sections were counterstained with the nucleic acid–binding dye DAPI (Vector Laboratories) to visualize the entire population of cell nuclei in the myocardial sections. To distinguish cardiomyocytes from nonmyocyte cell types, we further labeled myocardial sections with anti–desmin-rhodamine as previously described (4). Stained apoptotic myocyte nuclei were detected using a fluorescence microscope (×400; Nikon Eclipse E800; Nikon Instruments). Images were digitally photographed (SPOT II; Diagnostic Instruments) and analyzed with software that enabled us to enumerate cell nuclei (MetaView; Universal Imaging). Only those nuclei that were labeled with the ligase technique and were identified as cardiomyocytes were included in our quantification of cardiomyocyte apoptosis. In each microscopic field, the number of cardiomyocyte nuclei labeled by the in situ DNA ligation technique was divided by the total number of DAPI-stained nuclei. To quantify the prevalence of apoptosis, 3 LV cross-sections at the level of the papillary muscles were analyzed for each heart, for a total of 30 microscopic fields per heart.

Mechanisms for cardiomyocyte apoptosis: intrinsic pathway

Myocardial cytochrome c release. Whole hearts from 12-week-old mice were harvested, weighed, and immediately frozen. Cytosolic and mitochondrial proteins were isolated using a commercially available mitochondria/cytosol fractionating buffer system (BioVision). Protein concentrations were determined using the Bio-Rad protein assay (Bio-Rad). Equivalent amounts of mitochondrial (20 μg) and cytosolic (50 μg) myocardial protein extracts were separated on a 15% SDS-polyacrylamide gel and transferred to nitrocellulose membranes. Western blot analysis was performed using a polyclonal anti-mouse cytochrome *c* antibody (Santa Cruz Biotechnology Inc.) followed by a peroxidase-labeled secondary antibody. The antigen-antibody complexes were visualized by chemiluminescence (ECL; Amersham Pharmacia Biotech). Membranes were incubated at 70°C for 10 minutes in stripping buffer (10 mM Tris-HCl, pH 6.8, 2% SDS, 0.7% β-mercaptoethanol) then reprobed for GAPDH (Advanced Immunochemical) and COX IV (Molecular Probes) for loading normalization. Original films exposed to ECL (Hyperfilm, ECL; Amersham Pharmacia Biotech) were scanned on a Personal Densitometer S1 (Molecular Dynamics), and band density (measured in arbitrary units) was evaluated using ImageQuaNT 4.2a (Molecular Dynamics). Each sample value was normalized for loading errors and then

was divided by the mean value for the littermate controls. The resulting values within the same mouse group but from different blots were then combined. Thus group data express the fold difference of cytochrome *c* levels in transgenic animals (MHCsTNF, MHCsTNF/Bcl-2, and Bcl-2 mice) compared with wild-type (littermate control) animals (experimental/control).

Myocardial levels of proapoptotic proteins. Western blotting of cytosolic extracts was performed as described using the following antibodies: polyclonal anti-mouse Smac/Diablo (BioVision), polyclonal anti-mouse Omi/HtrA2 (R&D Systems), polyclonal anti-mouse AIF (Santa Cruz Biotechnology Inc.), and polyclonal anti-mouse Endo G (Abcam Inc.).

Myocardial caspase-3 and -9 activation. We performed fluorogenic assays for caspase-3– and caspase-9–like activity in the hearts of 12-week-old littermate control, MHCsTNF, MHCsTNF/Bcl-2, and Bcl-2 mice. Frozen hearts were homogenized in 500 μl assay buffer (caspase-3: 50 mM Hepes, pH 7.4, 100 mM NaCl, 0.1% Chaps, 10 mM DTT, 1 mM EDTA, 10% glycerol; caspase-9: 25 mM MES, pH 6.5, 100 mM NaCl, 0.1% Chaps, 10 mM DTT, 1 mM EDTA, 10% sucrose). Cells were allowed to swell on ice before cell debris was removed by centrifugation at 700 *g* for 10 minutes at 4°C. The supernatant was centrifuged again at 1,000 *g* for 10 minutes at 4°C and the pellet discarded. Caspase measurements were immediately performed on the supernatant using fluorogenic substrates specific for caspase-3–like (Ac-DEVD-afc) and caspase-9–like (Ac-LEHD-afc) cleavage (Biomol Research Laboratories). Briefly, 0.5 mg protein was incubated either with substrate or was pretreated with a specific inhibitor for caspase-3 (Ac-DEVD-CHO) or caspase-9 (Ac-LEHD-CHO) prior to adding the substrate. To eliminate background signal during the measurement of caspase-9 activity, 5 U/ml of casputin reagent (Biomol) was added to the assay reaction (32). Kinetic measurements were obtained at room temperature for 4 hours using a FLx800 Microplate Fluorescence Reader (excitation, 360/40 nm; emission, 530/20 nm; Bio-Tek Instruments). Measurements of caspase activity were determined from the steepest slope of the resulting curve, which was determined using KCjunior software (Bio-Tek Instruments). Each sample (with and without inhibitors) was measured in duplicate. The values obtained for noninhibitable protease cleavage were subtracted from the value of the same sample obtained without inhibitor pretreatment in order to obtain specific activity. Final values for caspase-3– and caspase-9–like activity were normalized by the total protein concentration for each sample.

Mechanisms for cardiomyocyte apoptosis: extrinsic pathway

Caspase-8 activation. Caspase-8–like activity was measured exactly as described above for caspase-3, except that we used Ac-IETD-afc as a fluorogenic substrate and Ac-IETD-CHO as the specific inhibitor (Biomol Research Laboratories).

Bid and IAPs. Cytosolic protein extracts were subjected to Western blotting using a polyclonal anti-mouse Bid antibody that detected both full-length and t-Bid and polyclonal anti-mouse c–IAP-1 and c–IAP-2 (all from Santa Cruz Biotechnology Inc.).

c-FLIP. Cytosolic protein extracts were subjected to Western blotting using polyclonal anti-mouse c-FLIP$_L$ and c-FLIP$_s$ antibodies (Kamiya Biomedical Co.). Total RNA was isolated from whole hearts using TRIZOL Reagent (Invitrogen), and levels of c-FLIP$_L$ mRNA were determined by a ribonuclease protection assay system using a custom-designed probe, according to the manufacturer's protocol (RiboQuant; BD Biosciences — Pharmingen) and described previously (33). Signals were quantified through the use of ImageQuaNT 4.2a (Molecular Dynamics Inc.) and were normalized to L32 expression.

Statistics

All data are expressed as mean ± SEM. Two-way ANOVA was used to evaluate the age- and mouse-dependent differences of LV dimensions, posterior wall thickness, and heart weight–to–body weight ratios. One-way ANOVA was used to test for mean differences in the prevalence of cardiomyocyte apoptosis, abundance of pro- and antiapoptotic proteins, and caspase-3–, caspase-8–, and caspase-9–like activities. Post-hoc testing (Student-Newman-Keuls method) was performed when appropriate. A P value of less than 0.05 was considered statistically significant.

Acknowledgments

We thank Thuy Pham and Claudia Aguillon for expert technical assistance. We thank Mark Entman for his critical review of the manuscript. This research was supported by research funds from the Veterans Administration and the NIH (P50 HL-O6H, RO1 HL58081-01, RO1 HL61543-01, and HL-42250-15/15 to D.L. Mann; AG-17899 to G.E. Taffet).

Received for publication September 18, 2006, and accepted in revised form May 29, 2007.

Address correspondence to: Douglas L. Mann, Faculty Center, 1709 Dryden Road, BCM620, FC 9.83, Houston, Texas 77030, USA. Phone: (713) 798-0285; Fax: (713) 798-0270; E-mail: dmann@bcm.tmc.edu.

1. Sivasubramanian, N., et al. 2001. Left ventricular remodeling in transgenic mice with cardiac restricted overexpression of tumor necrosis factor. *Circulation.* **104**:826–831.
2. Bryant, D., et al. 1998. Cardiac failure in transgenic mice with myocardial expression of tumor necrosis factor-α (TNF). *Circulation.* **97**:1375–1381.
3. Kubota, T., et al. 1997. Dilated cardiomyopathy in transgenic mice with cardiac specific overexpression of tumor necrosis factor-alpha. *Circ. Res.* **81**:627–635.
4. Engel, D., Peshock, R., Armstrong, R.C., Sivasubramanian, N., and Mann, D.L. 2004. Cardiac myocyte apoptosis provokes adverse cardiac remodeling in transgenic mice with targeted TNF overexpression. *Am. J. Physiol. Heart Circ. Physiol.* **287**:H1303–H1311.
5. Bishopric, N.H., Andreka, P., Slepak, T., and Webster, K.A. 2001. Molecular mechanisms of apoptosis in the cardiac myocyte. *Curr. Opin. Pharmacol.* **1**:141–150.
6. Foo, R.S., Mani, K., and Kitsis, R.N. 2005. Death begets failure in the heart. *J. Clin. Invest.* **115**:565–571. doi:10.1172/JCI200524569.
7. Tanaka, M., et al. 2004. Cardiomyocyte-specific Bcl-2 overexpression attenuates ischemia-reperfusion injury, immune response during acute rejection, and graft coronary artery disease. *Blood.* **104**:3789–3796.
8. Dimmeler, S., Breitschopf, K., Haendeler, J., and Zeiher, A.M. 1999. Dephosphorylation targets Bcl-2 for ubiquitin-dependent degradation: a link between the apoptosome and the proteasome pathway. *J. Exp. Med.* **189**:1815–1822.
9. Didenko, V.V., Tunstead, J.R., and Hornsby, P.J. 1998. Biotin-labeled haripin oligonucleotides: probes to detect double-strand breaks in DNA apopotic cells. *Am. J. Pathol.* **152**:897–902.
10. Chang, L., et al. 2006. The E3 ubiquitin ligase itch couples JNK activation to TNF alpha-induced cell death by inducing c-FLIP(L) turnover. *Cell.* **124**:601–613.
11. Mann, D.L., and Bristow, M.R. 2005. Mechanisms and models in heart failure: the biomechanical model and beyond. *Circulation.* **111**:2837–2849.
12. Yussman, M.G., et al. 2002. Mitochondrial death protein Nix is induced in cardiac hypertrophy and triggers apoptotic cardiomyopathy. *Nat. Med.* **8**:725–730.
13. Wencker, D., et al. 2003. A mechanistic role for cardiac myocyte apoptosis in heart failure. *J. Clin. Invest.* **111**:1497–1504. doi:10.1172/JCI200317664.
14. Hayakawa, Y., et al. 2003. Inhibition of cardiac myocyte apoptosis improves cardiac function and abolishes mortality in the peripartum cardiomyopathy of Galpha(q) transgenic mice. *Circulation.* **108**:3036–3041.
15. Communal, C., et al. 2002. Functional consequences of caspase activation in cardiac myocytes. *Proc. Natl. Acad. Sci. U. S. A.* **99**:6252–6256.
16. Chang, J., et al. 2003. Inhibitory cardiac transcription factor, SRF-N, is generated by caspase 3 cleavage in human heart failure and attenuated by ventricular unloading. *Circulation.* **108**:407–413.
17. Sun, X.M., et al. 2004. Caspase activation inhibits proteasome function during apoptosis. *Mol. Cell.* **14**:81–93.
18. Weisleder, N., Taffet, G.E., and Capetanaki, Y. 2004. Bcl-2 overexpression corrects mitochondrial defects and ameliorates inherited desmin null cardiomyopathy. *Proc. Natl. Acad. Sci. U. S. A.* **101**:769–774.
19. Green, D.R. 2000. Apoptotic pathways: paper wraps stone blunts scissors. *Cell.* **102**:1–4.
20. Micheau, O., and Tschopp, J. 2003. Induction of

TNF receptor I-mediated apoptosis via two sequential signaling complexes. *Cell.* **114**:181–190.
21. Peter, M.E., and Krammer, P.H. 2003. The CD95(APO-1/Fas) DISC and beyond. *Cell Death Differ.* **10**:26–35.
22. Donovan, M., and Cotter, T.G. 2004. Control of mitochondrial integrity by Bcl-2 family members and caspase-independent cell death. *Biochim. Biophys. Acta.* **1644**:133–147.
23. Zhu, L., et al. 1999. Modulation of mitochondrial Ca(2+) homeostasis by Bcl-2. *J. Biol. Chem.* **274**:33267–33273.
24. Zhu, L., Yu, Y., Chua, B.H., Ho, Y.S., and Kuo, T.H. 2001. Regulation of sodium-calcium exchange and mitochondrial energetics by Bcl-2 in the heart of transgenic mice. *J. Mol. Cell. Cardiol.* **33**:2135–2144.
25. Imahashi, K., Schneider, M.D., Steenbergen, C., and Murphy, E. 2004. Transgenic expression of Bcl-2 modulates energy metabolism, prevents cytosolic acidification during ischemia, and reduces ischemia/reperfusion injury. *Circ. Res.* **95**:734–741.
26. Kirshenbaum, L.A. 2000. Bcl-2 intersects the NFkappaB signalling pathway and suppresses apoptosis in ventricular myocytes. *Clin. Invest. Med.* **23**:322–330.
27. Hattori, R., et al. 2001. An essential role of the antioxidant gene Bcl-2 in myocardial adaptation to ischemia: an insight with antisense Bcl-2 therapy. *Antioxid. Redox Signal.* **3**:403–413.
28. Lee, L., Irani, K., and Finkel, T. 1998. Bcl-2 regulates nonapoptotic signal transduction: inhibition of c-Jun N-terminal kinase (JNK) activation by IL-1 beta and hydrogen peroxide. *Mol. Genet. Metab.* **64**:19–24.
29. Bradham, W.S., et al. 2002. TNF-alpha and myocardial matrix metalloproteinases in heart failure: relationship to LV remodeling. *Am. J. Physiol. Heart Circ. Physiol.* **282**:H1288–H1295.
30. Li, X., et al. 2000. Cardiac-specific overexpression of tumor necrosis factor-alpha causes oxidative stress and contractile dysfunction in mouse diaphragm. *Circulation.* **102**:1690–1696.
31. Nemoto, S., et al. 2002. Escherichia coli LPS-induced LV dysfunction: role of toll-like receptor-4 in the adult heart. *Am. J. Physiol. Heart Circ. Physiol.* **282**:H2316–H2323.
32. Beem, E., Holliday, L.S., and Segal, M.S. 2004. The 1.4-MDa apoptosome is a critical intermediate in apoptosome maturation. *Am. J. Physiol. Cell Physiol.* **287**:C664–C672.
33. Baumgarten, G., et al. 2001. In vivo expression of pro-inflammatory mediators in the adult heart after endotoxin administration: the role of toll-like receptor-4. *J. Infect. Dis.* **183**:1617–1624.